The Conformations of Filamentous and Soluble Tau Associated with Alzheimer Paired Helical Filaments †

ARTICLE *in* BIOCHEMISTRY · DECEMBER 2002

Impact Factor: 3.02 · DOI: 10.1021/bi016079h · Source: PubMed

1 AUTHOR:

Warren Goux
University of Texas at Dallas
64 PUBLICATIONS **1,587** CITATIONS

SEE PROFILE

The Conformations of Filamentous and Soluble Tau Associated with Alzheimer Paired Helical Filaments†

Warren J. Goux*

Department of Chemistry, The University of Texas at Dallas, P.O. Box 830688, Richardson, Texas 75080

Received December 20, 2001

ABSTRACT: Paired helical filaments (PHF) occur in Alzheimer's diseased brains and are known to be composed of the microtubule-associated protein, tau. In the present report, circular dichroism (CD) spectroscopy and transmission electron microscopy (TEM) were used to characterize PHF suspended in Tris-buffered saline (TBS), sodium acetate buffer, and water. In TBS the CD spectrum of PHF was observed to have a spectral pattern consistent with 31−37% α-helix, 15−20% β-sheet, 20−23% turn, and 26−29% unordered structure. The TBS sample was found to undergo a cooperative thermal transition between 70 and 75 °C, consistent with the changes observed in filament morphology, and it suggests that filamentous tau in the PHF (PHF-tau) makes a substantial contribution to the overall CD. Observed changes in the CD spectrum following removal of PHF by centrifugation suggest that PHF-tau possesses a higher fraction of α-helical structure than soluble tau. In acetate buffer, where only straight filaments were observed, the CD was consistent with a marked decrease in the fraction of α-helix and an increase in the fraction of β-sheet relative to the sample in TBS. In water, where only rudimentary filaments remain, the CD was consistent with a Type II or II′ β-turn conformation. Only noncooperative thermal transitions were observed for the PHF samples in acetate buffer and water, consistent with the presence of a heterogeneous population of folded structures. Taken cumulatively, the results are consistent with immunological data showing the presence of folded forms of tau and suggest that phosphorylation or nonproteinaceous components are able to induce conformations of tau other than the random coil conformation previously reported for cloned or purified human tau.

Paired helical filaments (PHF)[1] and a minor population of single straight filaments accumulate intraneuronally in the brains of AD patients and patients suffering from other neurodegenerative diseases such as frontotemporal dementias (collectively termed FTDP-17), progressive supranuclear palsy, and corticobasal degeneration (*1*, *2*). Investigations by electron microscopy shows that the PHF appear as two strands wound in a left-handed helical sense with a half-periodicity of 80 nm and a width alternating between 10 and 20 nm (*3*−*6*). Immunological and biochemical evidence suggests that PHF are composed of a hyperphosphorylated form of the microtubule-associated protein tau (*7*−*11*), closely associated with a unique glycolipid (*12*−*14*). Because phosphorylation appears to be the only posttranslational modification which distinguishes PHF-tau from normal tau, it has been suggested that phosphorylation of tau is prerequisite to its assembly into PHF. However, the mechanism by which assembly occurs remains controversial.

In vivo tau phosphorylation is regulated by the relative activity of cell kinases and phosphatases, and phosphorylated tau has been shown to have reduced affinity to microtubules (*15*−*18*). It has been proposed that PHF assembly in AD brain is a concentration-driven phenomenon, regulated by the binding stoichiometry of tau to microtubules. This proposal appears to correlate with the finding that tau is found in AD brain at 8 times the concentration of that in normal brain (*19*). In addition, it has been proposed that phosphorylation of tau may lead to an altered conformational state of the protein catalytic in PHF formation. This theory is supported by biophysical evidence showing that (1) tau paracrystals become longer and stiffer following phosphorylation (*20*), suggesting a conformational change of the protein upon phosphorylation and (2) NMR and CD evidence which shows that a tau peptide undergoes a conformational change following phosphorylation at Thr231 and Ser235 (*21*).

Although there is much evidence which supports the theory that tau phosphorylation is prerequisite to PHF assembly, alternative evidence exists which suggests that phosphorylation of tau is circumstantial and plays a minor role in the mechanism by which PHF assembly occurs. One of the more compelling lines of evidence for this latter argument is that nonphosphorylated full-length human tau and tau peptides are able to form PHF-like filaments in vitro in the presence of a catalyst such as a polyanion or unsaturated fatty acid (*22*−*28*). A second line of evidence is based on the immunoreactivity of tau with a group of "conformation-

† The author acknowledges The National Institutes on Aging for their financial support (NIA 1R03AG16042-01).

* E-mail: wgoux@utdallas.edu.

[1] Abbreviations: SDS, sodium dodecyl (lauryl) sulfate; PAGE, polyacrylamide gel electrophoresis; CD, circular dichroism; PHF, paired helical filaments; TBS, Tris-buffered saline; TEM, transmission electron microscopy; FTDP-17, frontotemporal dementia; PHF-TBS, PHF in Tris-buffered saline; PHF-Ac, PHF in sodium acetate; PHF-H_2O/TBS, PHF in water dialyzed from TBS; PHF-H_2O/Ac, PHF in water dialyzed from sodium acetate; PHF-tau, filamentous tau in PHF; FTIR, Fourier transform infrared spectroscopy; NMR, nuclear magnetic resonance, C-terminal, carboxy-terminal.

10.1021/bi016079h CCC: $22.00
Published on Web 10/17/2002

dependent" monoclonal antibodies whose immunoreactivity depends on simultaneous binding to tau epitopes in distant parts of the sequence and not on the phosphorylation state of tau per se (*29*−*32*). The finding that these antibodies react with non-PHF tau from biopsied AD brain but not from normal brain suggests that tau assumes an altered conformation in AD brain before it aggregates into PHF (*30*).

The helical symmetry of PHF suggests that PHF-tau assumes significant secondary and tertiary structure and that there exists regular contacts between protein monomers within the superstructure. If, as studies with conformation-dependent antibodies suggest, there is a conformation of soluble tau unique to AD, then it is reasonable to assume that its conformation resembles filamentous tau in PHF. However, early biophysical studies on bovine tau and cloned human tau showed that the predominant conformation in solution was consistent with that of a random coil (*33*, *34*). The picture becomes more complex when more recent data for tau, tau peptides, or FTDP-17 mutants of tau are considered. Jicha et al. (*35*) reported that the CD of some of the FTDP-17 tau mutant proteins resembled those of proteins having a high abundance of α-helical structure. Under conditions which induce filament formation, cloned human tau was found to have a CD which suggested the presence of β-sheet structure (*36*), an interpretation which has recently been verified by FTIR data for helical filaments formed from FTDP-17 mutant tau and tau peptides (*27*, *28*, *36*). In a recent report, CD and FTIR were used to show that PHF isolated from AD brain possess 70−80% α-helical structure (*37*).

In the present study, CD is used to characterize the conformation of tau in PHF preparations in water and two different buffer systems. The CD features displayed and their temperature dependence were unique to each of the different forms of tau characterized and suggest that a heterogeneous population of tau conformers gives rise to the CD. The results provide the first physical evidence that substantiate immunological claims that soluble PHF-tau assumes folded conformations (*29*−*32*) and suggest that PHF-tau may be affected by hyperphosphorylation or by other nonproteinaceous components, leading to conformations other than the random coil conformations previously determined (*33*, *34*).

EXPERIMENTAL PROCEDURES

Materials. Mouse monoclonal τ-1 antibody was obtained from Boehringer-Mannheim (Indianapolis, IN), and biotinylated goat anti-mouse secondary antibody was obtained from Bio-Rad Laboratories (Hercules, CA). Goat polyclonal antibody to the N-terminal amino acids 1−16 of human tau was provided by Southwest Immunology, Inc. (Ennis, Texas). Anti-goat antibody conjugated to 5 nm gold particles was obtained from Sigma Chemical (St. Louis, MO). Avidin and biotinylated horseradish peroxidase were obtained from Pierce Endogen (Rockford, IL). All other chemicals were of reagent grade and were used without further purification.

PHF. Immunoaffinity-purified PHF samples, prepared according to previously published procedures (*38*, *39*), were a gift of Dr. Peter Davies (Albert Einstein College of Medicine). A 0.3 mL aliquot of the PHF sample in 10 mM Tris, 0.15 M sodium chloride, pH 7.4 (TBS), was dialyzed at 4 °C against three 1 L changes of deionized water or 5 mM sodium acetate, pH 6.8. A final PHF sample was prepared by dialysis of PHF in sodium acetate into deionized water. One PHF sample in TBS was prepared following centrifugation at 100 000*g* for 1 h.

Initially, protein concentrations were measured by a colorimetric microassay method (DC Protein Assay, Bio-Rad Laboratories). However, in previous work it was noted that the fibrous nature of the PHF samples and any associated glycolipid are likely to lead to errors in the determination of tau concentration (*12*). For these reasons, protein concentrations were redetermined by amino acid analysis. Following the acquisition of CD spectra, 1 nmol of γ-amino butyric acid (Abu) was added to the sample. The sample was lyophilized to dryness and hydrolyzed with 6 M HCl overnight at 110 °C in a sealed evacuated reaction vessel. Analysis was carried out using a Waters ACQ-Tag amino acid analysis system (Waters Corp., Milford, MA). Amino acids, except for tryptophan and cysteine, were quantitated with respect to the Abu internal standard, taking into account appropriate response factors. Concentrations determined by the acid hydrolysis method were found to be between 5% and 15% lower than those initially determined by the colorimetric method.

Electron Microscopy of PHF. Samples for transmission electron microscopy were prepared by floating a Formvar carbon-coated copper grid on a 10 μL drop of the sample for 10 min. The sample was then negatively stained for 2 min with 1% uranyl acetate, rinsed one time with deionized water, and wicked dry. A JEOL 1200 EX scope interfaced to a digital camera was used to visualize samples.

For colloidal gold studies, the sample-loaded grids were blocked with 0.5% bovine serum albumin in TBS, pH 8.2 (TBS/BSA), for 10 min at room temperature. The primary goat anti-τ antibody was diluted 1:50 in TBS/BSA and the grids floated sample side down on a drop for 30 min. The grids were washed for 10 min by transferring to drops of TBS then transferred to colloidal gold conjugated anti-goat antibody diluted 1:10 in TBS/BSA. The grids were washed 5 min in TBS, 5 min in deionized water and then stained with 1% uranyl acetate, as described above.

PAGE Electrophoresis and Immunoblotting. Electrophoresis was carried out using 8 cm 10% polyacrylamide gels with a 4% stacking gel according to Laemmli (*40*). The proteins were visualized in the gel by silver staining or electrophoretically transferred to 0.45 μm nitrocellulose for immunoblotting. The blots were blocked 1 h in 3% BSA in 10 mM sodium phosphate, 0.15 M sodium chloride containing 0.1% Tween-20 (PBST), pH 7.2, and then incubated overnight in a 1:500 dilution of τ-1 antibody in PBST containing 1% BSA. The blots were washed three times in PBST, incubated 1 h in a 1:500 dilution of biotinylated goat anti-mouse antibody, washed again, and then incubated in a 1:500 dilution of avidin and biotinylated horseradish peroxidase for 30 min. After an additional wash, the reactive proteins were visualized by reaction with 4-chloronaphthal in peroxide.

CD Spectroscopy. CD spectra were acquired on an AVIV Model 202 spectropolarimeter using a 0.1 cm path length quartz cell. Temperature was controlled with an electrothermal cell holder, and the sample was equilibrated 5 min prior to spectral acquisition. Spectra, reported as an average of 16 scans, were smoothed using AVIV software employing

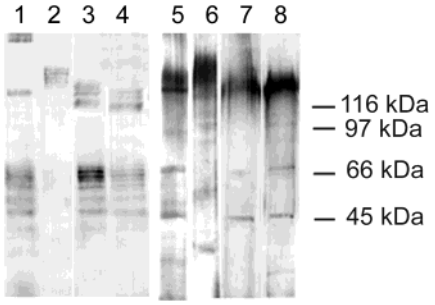

FIGURE 1: SDS-PAGE of PHF initially suspended in TBS, pH 7.4, 5 mM sodium acetate, pH 6.8, water dialyzed from sodium acetate, and water dialyzed from TBS, visualized with τ-1 antibody (*lanes 1*−*4*) and with silver staining (*lanes 5*−*8*).

an 11-data point running average and converted to mean residue ellipticity assuming a molecular weight of 45 kDa and 441 residues (full-length tau). Scattering, as judged by the response in the absorbance spectrum at wavelengths longer than 300 nm, was negligible at the protein concentrations used for the CD experiments.

Estimates of secondary structure were made using the CDPro suite of programs (*41*, *42*). Each of the three programs within the suite, SELCON3, CONTINLL, and CDSSTR uses slightly different algorithms to minimize the difference between the experimental CD and a linear combination of CD spectra contained in the reference data set. Experimental CD spectra between 185 and 240 nm were fit to a reference set of CD spectra of 37 proteins of known secondary structure. Alternatively, cluster analysis was used to select a smaller subset of reference proteins based on the tertiary structure (*42*).

RESULTS

Figure 1 shows the SDS−PAGE of PHF in TBS, pH 7.4, PHF in 5 mM sodium acetate, pH 6.8, PHF in water dialyzed from TBS, and PHF in water dialyzed from sodium acetate. Western blots of PHF in TBS (PHF-TBS) developed with τ-1 antibody show well-defined bands at 54, 60, 64, and 68 kDa for the monomeric phosphorylated tau isoforms, in addition to some high molecular weight aggregation products (134, 205, and 215 kDa) (lane 1). The pattern of three bands at 60, 64, and 68 kDa has previously been observed for PHF-tau and confirm the hyperphosphorylated state of the protein (*11*, *43*). Additional bands are visible, appearing as lower molecular weight bands at 41 and 48 kDa. These bands have previously been attributed to C-terminal tau degradation products on the basis of their immunoreactivity (*32*). The SDS−PAGE of PHF in sodium acetate (PHF-Ac) shows that the majority of the protein migrates as a series of four bands at 145, 150, 157, and 162 kDa, with only a minor fraction of the protein migrating as monomeric isoforms. High molecular weight bands are also visible for PHF in water dialyzed from sodium acetate (PHF-HF-H_2O/Ac) (at 121, 131, 138, and 141 kDa) and PHF in water dialyzed from TBS (PHF-H_2O/TBS) (at 120, 128, and 135 kDa). Blots of PHF-H_2O/Ac and PHF-H_2O/TBS also display a series of tau bands between 52 and 68 kDa and bands at 41 and 48 kDa arising from tau degradation products. The similarity of the pattern of high molecular weight bands to those observed for monomeric tau and the fact that the calculated molecular weights of these bands are approximately twice those of tau monomers suggests that the bands between 120 and 145 kDa arise from tau dimers. Irrespective of the buffer in which the PHF were originally suspended, bands for PHF appearing in the Western blots also appear in the silver-stained gel, although with reduced definition. While the band for the tau monomer at 68 kDa and at 48 kDa for the tau degradation product are darkly stained, other bands between 52 and 68 kDa appear poorly defined. However, no bands appear in the silver-stained gel which are not in the Western blot, indicating the absence of nontau protein.

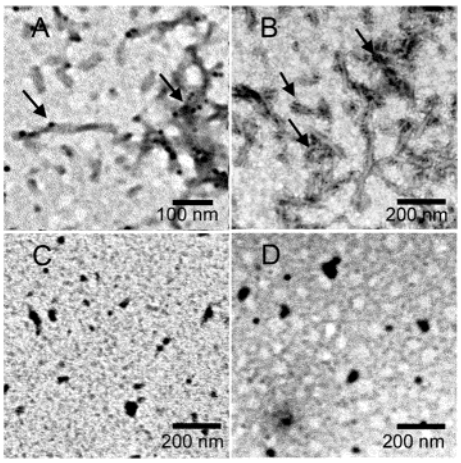

FIGURE 2: Transmission electron micrographs of (A) PHF in TBS, pH 7.4, (B) PHF in 5 mM sodium acetate, pH 6.8, (C) PHF in water dialyzed from TBS, and (D) PHF in water dialyzed from sodium acetate. The samples were immunostained with colloidal gold (5 nm) using goat polyclonal anti-τ as the primary antibody. Arrows in panels A and B point to colloidal gold bound to the filaments.

Electron micrographs of the PHF preparations immunostained with an anti-τ antibody are shown in Figure 2. Colloidal gold particles are seen to decorate the filaments in the PHF-TBS and PHF-Ac preparations. While the filaments in both of these preparations show 26 nm wide filaments, those in the TBS preparation have a defined left-handed helical twist, which is absent in filaments in sodium acetate. There were no filaments observed in PHF preparations in water. Micrographs of these preparations show the immunogold particles localize in small regions, consistent with either pieces of disintegrated filaments or sites of filament nucleation.

Figure 3 shows the CD spectra of PHF-TBS, PHF-TBS following centrifugation, PHF-Ac, PHF-H_2O/Ac, and PHF-H_2O/TBS. The CD spectra of both PHF-TBS and PHF-Ac display a positive maximum at 192 nm, a negative maximum at 209 nm, and a negative shoulder at 219 nm, but with the bands for PHF-Ac less intense than those of PHF-TBS. The spectra differ from those previously reported for isolated tau protein (*33*, *34*, *44*), cloned full-length human tau (*34*, *36*), or tau peptides (*34*, *36*, *45*, *46*), all of which display a minor negative shoulder at about 220 nm and a strong negative maximum between 195 and 200 nm, a spectral pattern characteristic of a random coil or a left-handed polyproline II helix (*47*−*49*). On the other hand, the CD spectra observed for PHF-TBS and PHF-Ac appear similar to those previously reported for some mutants of full-length tau associated with FTDP-17 (*35*). The spectra for PHF-TBS and PHF-Ac could be fit to spectra representative of secondary structural elements using the CDPro suite of programs (*41*, *42*), and

Table 1: Results for the CDPro Program Suite for PHF in TBS and Sodium Acetate Buffer[a]

species[b]	ref set	program	H(r)	H(d)	S(r)	S(d)	T	U	rms
PHF-TBS	37	CDSSTR	0.19	0.14	0.12	0.08	0.20	0.26	0.11
PHF-TBS	37	CONTINLL	0.18	0.14	0.10	0.07	0.22	0.29	0.07
PHF-TBS	37	SELCON3	0.18	0.14	0.08	0.08	0.22	0.29	0.28
PHF-TBS	CA	CDSSTR	0.20	0.14	0.11	0.08	0.19	0.28	0.08
PHF-TBS	CA	CONTINLL	0.21	0.16	0.08	0.07	0.20	0.28	0.04
PHF-TBS	CA	SELCON3	0.17	0.14	0.09	0.08	0.23	0.28	0.16
PHF-Ac	CA	CDSSTR	0.03	0.05	0.28	0.12	0.20	0.31	0.07
PHF-Ac	CA	CONTINLL	0.03	0.05	0.28	0.12	0.21	0.30	0.04
PHF-Ac	CA	SELCON3	0.03	0.04	0.28	0.12	0.21	0.30	0.07
PHF-Ac	37	CDSSTR	0.02	0.05	0.26	0.12	0.23	0.32	0.13
PHF-Ac	37	CONTINLL	0.11	0.12	0.20	0.09	0.19	0.27	0.02
PHF-Ac	37	SELCON3	0.04	0.07	0.26	0.12	0.21	0.30	0.20

[a] CDPro uses programs CDSSTR, CONTINLL, and SELCON3 to fit experimental CD to a reference set of CD spectra of 37 proteins of known secondary structure between 185 and 240 nm (*41*, *42*). Alternatively, cluster analysis (CA) was used to select a smaller subset of reference proteins based on the tertiary structure determined from the experimental CD spectrum. [b] Ref set, reference set used to fit the experimental CD spectrum; H(r), regular α-helix; H(d), distorted α-helix; S(r) regular β-strand; S(d), distorted β-strand; T, turns; U, unordered; RMS, root-mean-square deviation between experimental and calculated CD spectrum.

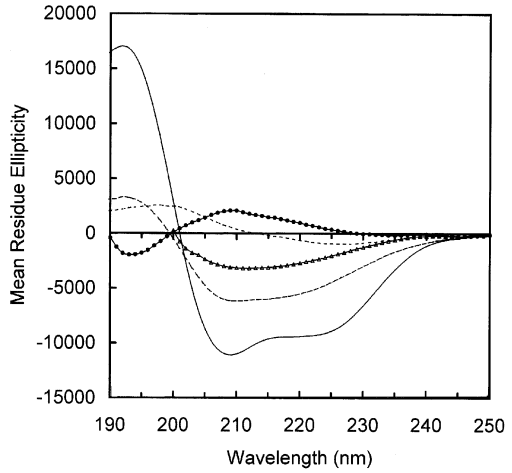

FIGURE 3: CD spectra of PHF preparations in TBS, pH 7.4 (—), in TBS following centrifugation (▲), in 5 mM sodium acetate, pH 6.8 (---), in water dialyzed from TBS (●), and in water dialyzed from sodium acetate (•••). All spectra were acquired at 20 °C.

these results are summarized in Table 1. Spectra were fit to a reference set containing 37 proteins of known secondary structure or to a smaller subset selected on the basis of cluster analysis (*42*). In the case of PHF-TBS, all three program packages contained in the CDPro suite yielded estimates between 31% and 37% helix, 15% and 20% β-sheet, 20% and 23% turn, and 26% and 29% unordered structure, irrespective of the reference set used. Five of six calculations resulted in estimates of 7−11% helix, 38−40% β-sheet, 20−23% turn, and 30−32% unordered structure for PHF-Ac.

The CD spectrum of PHF-H_2O/TBS and PHF-H_2O/Ac are markedly different from those of PHF-TBS or PHF-Ac. While the CD of PHF-H_2O/TBS displays a low-intensity minimum between 235 and 240 nm, a positive band at 212 nm, and a negative minimum at 192 nm, the CD of PHF-H_2O/Ac has a negative minimum at 227 nm and a broad positive band between 199 and 203 nm. The CDPro software was unable to fit either the PHF-H_2O/TBS or the PHF-H_2O/Ac CD spectra. Woody has used a perturbation matrix theory approach to calculate CD spectra arising from β-turn structures and found that five types of spectra may result, depending on minor changes of the dihedral angles defining the β-turn (*50*). Two of these spectra, type B, having a negative nπ* band red shifted above 220 nm and the positive band of a $\pi\pi$* couplet between 200 and 210 nm, and type C′, having a positive $\pi\pi$* band at 210 nm, a positive nπ* shoulder at 220 nm, and a negative $\pi\pi$* band at about 190 nm, resemble those observed for PHF-H_2O/Ac and PHF-H_2O/TBS, respectively. On the basis of this resemblance, features of β-turn spectra are believed to dominate the CD spectra of these PHF preparations.

Figure 4 shows the temperature dependence of the CD for the four PHF forms studied. At temperatures above 10 °C, all of the bands in the spectrum of PHF-TBS become less intense, with the decrease most pronounced between 70 and 80 °C (Figure 4A). The presence of the isodichroic point at 202 nm suggests the presence of a two-state transition between a native and a denatured form of the protein (*49*, *51*). The CD spectrum does not return to that of the native protein after heating to elevated temperatures, suggesting that the denaturation process is irreversible. A plot of the ellipticity at 209 nm as a function of temperature shows that the protein in the TBS preparation has a well-defined transition temperature between 70 and 75 °C (Figure 5A).

To correlate the temperature-dependent changes seen in the CD spectrum of PHF-TBS with changes in filament morphology, the preparation was heated to 90 °C, well above the transition temperature, and incubated for increasing periods of time. Electron micrographs show that after only 1 min the PHF begin to aggregate and aggregation continues until only fibrous sheets appear following a 5 min incubation (Figure 6). Hence, it appears that protein unfolding seen in the CD occurs concomitantly with unraveling of the PHF.

The apparent correlation of the temperature dependence of the CD of PHF-TBS with changes in filament morphology observed at elevated temperatures suggests that a significant contribution to the CD comes from PHF-tau. In an attempt to verify this proposal by an independent method, the CD of the supernatant fraction was recorded following centrifugation of PHF-TBS. The spectrum of the supernatant fraction appears qualitatively similar to the CD spectrum of PHF-Ac and is decreased in intensity 4-fold compared to the spectrum of PHF-TBS (Figure 3). Fitting of the spectrum using the CDPro package yielded results similar to those for PHF-Ac (5−6% helix, 35−39% β-sheet, 21−24% turn and 30−33% unordered structure). This result suggests that the observed CD of PHF-TBS arises from a weighted average

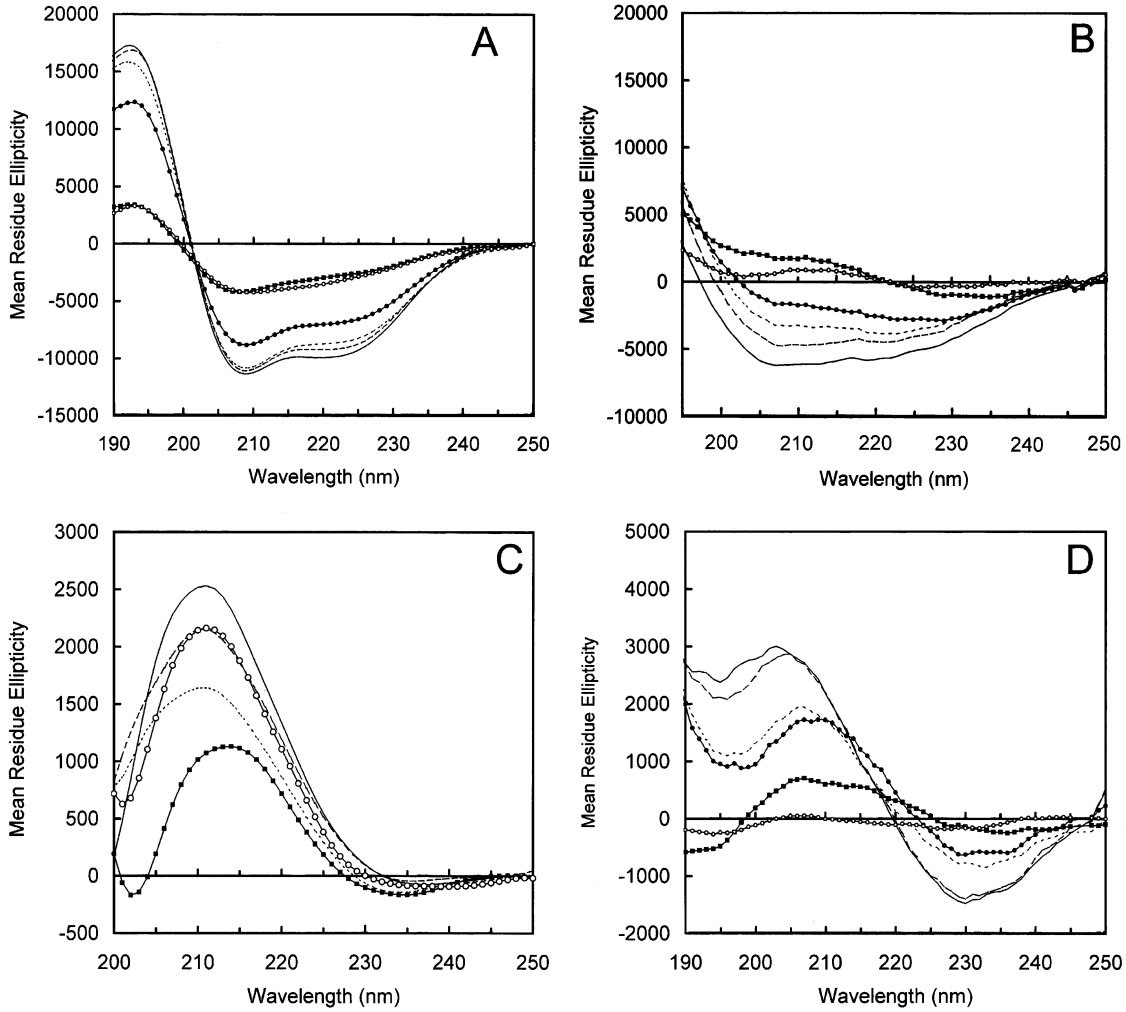

FIGURE 4: CD spectra of (A) PHF in TBS, pH 7.4, at 10 (—), 40 (---), 60 (···), 70 (●), 80 (■), and 25 °C after heating to 80 °C (○); (B) PHF in 5 mM sodium acetate, pH 6.8, at 25 (—), 40 (---), 50 °C (···), 60 (●), 80 (■), and 25 °C after heating to 80 °C (○); (C) PHF in water, dialyzed from TBS, pH 7.4, at 20 (—), 30 (---), 45 (···), 75 (■), and 30 °C after heating to 80 °C (○); (D) PHF in water, dialyzed from 5 mM sodium acetate, pH 6.8, at 25 (—), 40 (---), 55 (···), 60 (●), 80 (■), and 25 °C after heating to 80 °C (○).

of PHF-tau and soluble tau, with the PHF-tau containing a larger fraction of α-helical structure relative to soluble tau. However, because no independent method exists by which the fraction of filamentous tau in the supernatant can be estimated, CD spectra of the fractions present in the sample cannot be independently determined.

With increasing temperature, the negative bands at 209 and 219 nm in the CD spectrum of PHF-Ac become increasingly positive (Figure 4B). Above 80 °C a new positive band appears at 213 nm, and except for the absence of the negative band at 192 nm (as seen in Figure 3), the spectrum resembles the type C′ spectrum seen for the PHF-H_2O/TBS. These temperature-dependent changes suggest that the decreased intensity of the 209 and 219 nm bands relative to those of PHF-TBS at 20 °C are due to a positive contribution from a type C′ spectrum. Conversely, the absence of the negative 192 nm band in the CD of PHF-Ac at 80 °C is probably due to a positive contribution at lower wavelength. Following heating to elevated temperatures, the CD of the protein at ambient temperature does not revert to the spectrum observed for PHF-Ac at 25 °C, prior to heating. A plot of the ellipticity at 209 nm as a function of temperature shows there to be no defined cooperative thermal transition (Figure 5A). This result is consistent with either the denaturation of several tau forms or the denaturation of a single most abundant form, loosely folded at ambient temperature.

Figure 4C shows that as PHF-H_2O/TBS is heated there is a decrease in the 212 nm positive band and, at temperatures above 70 °C, the band is red shifted about 2 nm. Return to 30 °C after heating to elevated temperatures yields a CD spectrum nearly identical to the spectrum at 30 °C, prior to heating. A plot of ellipticity at 212 nm verses temperature shows that there is no cooperative transition (Figure 5B).

The CD of PHF-H_2O/Ac undergoes complex changes with increasing temperature (Figure 4D). The negative band at about 230 nm decreases in intensity, while the lower wavelength positive band also decreases in intensity and is red shifted. The absence of a defined isodichroic point suggests a complex denaturation process and the absence of any measurable CD after cooling the protein to ambient temperatures is consistent with an irreversible process. A plot of the ellipticity at 230 nm as a function of temperature also shows complex behavior (Figure 5B). The data may be fit to a single broad thermal transition between 50 and 55 °C and suggest a multiple step transition to the denatured form of a single protein or denaturation of two or more forms of tau.

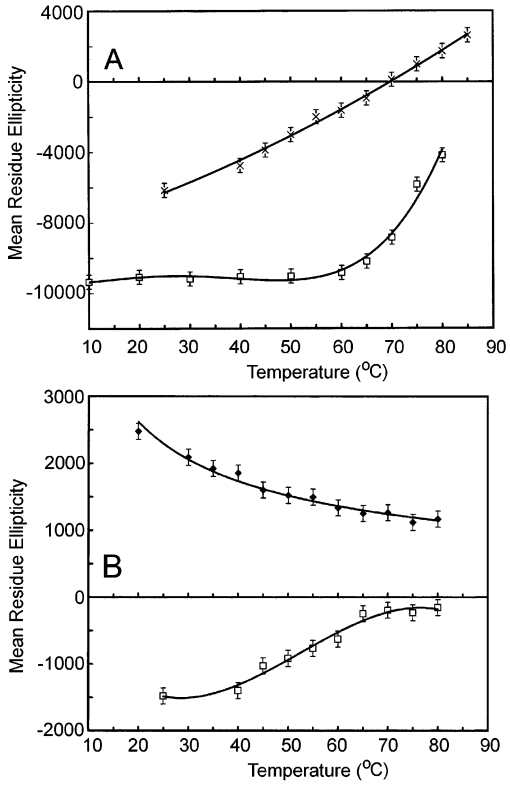

FIGURE 5: Temperature dependence of the CD of (A) PHF in TBS, pH 7.4 (□), and PHF in 5 mM sodium acetate, pH 6.8 (×), at 209 nm, and (B) PHF in water dialyzed from TBS, pH 7.4 (◆), at 212 nm and PHF in water dialyzed from 5 mM sodium acetate, pH 6.8 (□), at 230 nm. Error bars were estimated from the noise present in the original data prior to smoothing. Lines in the data represent best-fit polynomial functions.

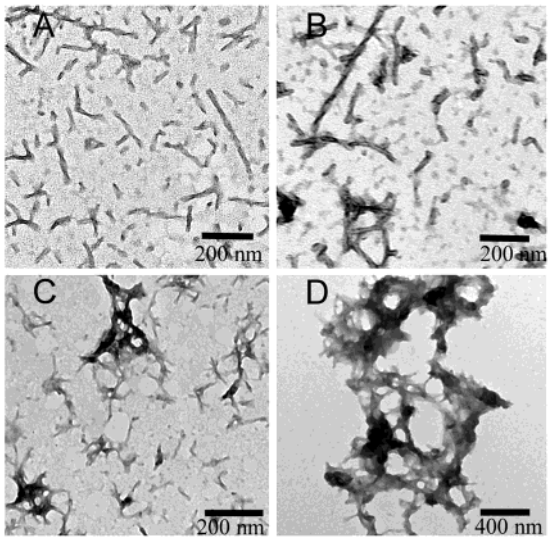

FIGURE 6: Electron micrographs of PHF in TBS, pH 7.4, following incubation at 90 °C for (A) 0, (B) 1, (C) 2, and (D) 5 min. Samples were negatively stained with 1% uranyl acetate.

DISCUSSION

The SDS−PAGE of PHF in TBS shows a set of bands between 54 and 68 kDa, previously attributed to the phosphorylated isoforms of monomeric tau (*11*). The data could suggest that the majority of filamentous tau is disaggregated to a monomeric denatured form upon heating the PHF in SDS-containing loading buffer. A minor fraction, observed as a broad band at greater than 200 kDa, can be attributed to a fraction of nondenatured tau in PHF. An alternative interpretation is that soluble tau exists in equilibrium with filamentous tau and that heating in loading buffer, while producing the desired denaturation and binding of SDS to the soluble form of tau, converts the PHF in the sample to a more highly aggregated form. This latter interpretation is consistent with the highly aggregated forms of PHF observed in electron micrographs following heating of samples in TBS for short periods of time.

When the PHF samples are dialyzed into water, only rudimentary filaments remain (Figure 2C and 2D), due either to the fragments of the PHF once present or nucleation fragments for new filaments formed from the soluble tau present in solution. A set of bands appear in the SDS−PAGE of samples of PHF in water (either dialyzed from sodium acetate or from TBS) and PHF in sodium acetate at 120−160 kDa, roughly twice the molecular weight as the phosphorylated tau monomers. It is possible that oxidative cross-linking of tau monomers in the PHF preferentially occurs in buffers of low ionic strength. Air oxidation of cysteines to disulfides to yield dimers has previously been observed for cloned tau in the absence of reducing agent (*52*).

The CD spectrum reported for PHF in TBS buffer have a CD spectrum which could be fit to a structure containing 31−37% helix, 15−20% β-sheet, 20−23% turn, and 26−29% unordered structure. Previous work has shown the CD spectra of cloned tau and phosphorylated cloned tau both to be consistent with predominantly unordered structures (*34*, *36*, *53*), while work with monoclonal antibodies verifies the existence of a population of folded conformations of tau in AD brain distinct from those found in normal brain (*29*−*32*, *54*). Amyloid fiber formation in other diseases arises when otherwise normally folded proteins assume a population of partially unfolded conformations (*55*), and it would not be unexpected that tau also populates a range of folded structures which may be perturbed by changes in temperature, pH, or ionic strength. Recent evidence for this is provided by the fact that tau immunoreactivity to a conformation-dependent monoclonal antibody is sensitive to temperature and buffer conditions (*54*). Hence, the fractions of secondary structures calculated by fitting the PHF CD spectra should be viewed with caution, as they likely represent structures present in a population of various folded tau monomers, tau aggregates, and filamentous tau. That a substantial fraction of the CD of PHF in TBS arises from filamentous tau is suggested by the fact that (1) the temperature dependence of the CD showed a cooperative transition between 70 and 75 °C, consistent with filament denaturation, (2) the spectrally observed thermal transition was consistent with changes observed in PHF morphology above the denaturation temperature, and (3) a significant decrease in the CD was observed following removal of the PHF by centrifugation, conditions under which filamentous tau would be expected to pellet out of solution.

The fraction of helical structure was found to decrease from roughly 35% in PHF-TBS to about 10% in PHF-Ac, while the fraction of β-sheet increased from about 15% in PHF-TBS to about 35% in PHF-Ac. It is interesting that estimates of secondary structure in the supernatant fraction of PHF-TBS following centrifugation are similar to those

for PHF in acetate buffer. There were no filaments observed in PHF samples in water, and it is likely that the filament population is substantially decreased in the low ionic strength acetate buffer and in the supernatant fraction. This being the case, it may be argued that the PHF-tau fraction possesses a higher fraction of α-helical structure and a lower fraction of β-sheet than soluble tau. The shape of the denaturation curve (Figure 5A) suggests a complex transition to the final state, which may result from the simultaneous denaturation of filaments and soluble forms of tau. The absence of filaments following heating of the PHF in sodium acetate (results not shown) suggests that the CD spectrum prior to heating arises predominantly from the PHF component and that the observed CD after cooling arises from soluble nonfilamentous forms of tau.

A working hypothesis which can be drawn from the fitting and temperature dependence data is that a variety of both soluble and filamentous structures contribute to the CD of PHF in TBS, the supernatant of the centrifuged PHF in TBS, and PHF sodium acetate. Furthermore, filamentous tau appears to make a greater helical-like contribution to the CD spectrum. This hypothesis makes possible the reinterpretation of previous CD data on cloned tau proteins and peptides capable of forming filaments. When polyanion effectors are added to cloned human tau protein or to tau peptides from the third repeat region in order to induce filament formation, the lower wavelength minimum at 200 nm is shifted to about 210 nm, and a negative nπ^* shoulder appears near 220 nm (*36*), a spectrum consistent with the spectrum observed for filamentous tau in the PHF-TBS preparation. In the absence of a polyanion effector, CD data suggest that greatest fraction of purified tau exists in a random coil or a polyproline II conformation (*33*−*36*), but does not eliminate the presence of a minor fractions of tau in different conformational states. Barghorn et al. (*27*) have reported CD consistent with a random coil conformation for all tau FTDP-17 mutants studied while Jicha et al. (*35*) reported CD of some of the FTDP-17 mutants (G272V, P301L, V337M, and R406W) to have a spectrum, consistent with a helical conformation. This discrepancy can be resolved if it is proposed that some of the FTDP-17 samples of Jicha et al. contained a significant fraction of filaments.

The CD of PHF in water, dialyzed from acetate or TBS, resemble type B and C′ spectra previously calculated by Woody for β-turn structures (*50*) and is similar to the CD of elastin above the coacervation temperature (*56*) or the C-terminal domain of the largest subunit of RNA polymerase II in trifluoroethanol (*57*), where spectral features characteristic of β-turn structure dominate the CD. The inability of the CDPro software to fit these spectra can be explained by the absence of representative spectra in the reference data sets. Since no filaments were observed in these samples, the CD must arise from the remaining population of tau conformers still present in solution. The lack of cooperativity observed in the temperature transitions of these samples suggests that a soluble fraction is made up of a distribution of loosely folded tau conformers.

On the basis of predicted secondary structure, the features seen in the CD of PHF in water attributable to β-turn seem reasonable. Tau is a relatively hydrophilic protein with a high abundance of glycine (20%), glutamate/glutamine (12%), serine (8%), and proline (9%) (*58*). The protein is rich in Ser(Thr)−Pro motifs, known to be substrates for Ser(Thr)−Pro directed kinases (*16*). In fact, tau possesses the Ser(Thr)−Pro motif at roughly 6 times the frequency of gene regulatory proteins where the SPXX motif serves as a DNA binding sequence (*59*). Previous studies have shown that proline is frequently involved in a β-turn by reason of its restricted ϕ angle and that the Pro-Gly motif is favored to make a Type II β-turn, with the NH of residue ($i + 3$) stabilizing the turn structure by hydrogen bonding with the CO of residue *i*. The SPXX motif is known to stabilize β-turns, independent of X, since the serine side chain hydroxyl at position *i* is able to form an additional hydrogen bond with the NH of residue ($i + 1$), stabilizing a Type I β-turn. The Chou-Fasman algorithm predicts tau contains 54 β-turns involving about 35% the protein sequence (*60*). Many of the predicted turns occur in the proline-rich region upstream of the microtubule-binding region, roughly between residues 150 and 250. An analysis of the predicted secondary structure probabilities as a function of sequence shows that high turn probability is also predicted for PGGG sequences which terminate each of the four homologous 32 amino acid repeats in the microtubule binding region. Pockets of β-sheet are predicted immediately following these PGGG motifs around residues 274 and 309, and it has recently been demonstrated that peptides which include these sequences are able to form filaments in vitro (*27*, *28*, *36*).

Studies with model peptides suggest that Type I turns give rise to a type C spectrum, similar to that observed for PHF in TBS, Type II turns give rise to a type B spectrum, similar to that observed for PHF in water dialyzed from sodium acetate, and Type II′ turns give rise to a type C′ spectrum, similar to that observed for PHF in water dialyzed from TBS (*61*−*63*). Furthermore, the type of β-turn structure may be determined by cis−trans isomerization around the X-Pro bond. Turns involving cis proline at the ($i + 1$) or the ($i + 2$) positions give rise to Type I or Type II′ turns, while those involving trans proline at the ($i + 1$) position give rise to Type II turns (*61*). It may be that for tau, a protein rich in proline-containing sequences, temperature- or solvent-induced changes in the cis−trans proline distribution of isomers results in a change in protein conformation and the observed CD. In this respect it is particularly relevant that a proline isomerase, Pin1, has been found to bind in the proline-rich region, near Thr231-Pro232, where β-turn probability is high (*64*). It may be that under normal physiological conditions, Pin1 induces a conformational transition in tau which initiate its self-association into PHF.

In summary, the results of the present study suggest that (1) the fractions of soluble tau and PHF-tau present are effected by the ionic strength of the buffer system and these changes are reflected in the CD spectrum, (2) the tau present as PHF contains a higher fraction of α-helical structure than soluble tau, and (3) the soluble tau present in PHF preparations may exist in conformations other than random coil. The CD of PHF in distilled water suggests that a distribution of protein conformers exists which contains a significant fraction of β-turn structure.

During the time this manuscript was in review, a publication appeared by Sadqi et al. on the spectroscopic properties of PHF in 20 mM phosphate buffer (*37*). On the basis of CD and FTIR data, the authors estimate that greater than 70% of tau in PHF exists in an α-helical conformation. The

results of the present study suggest that tau in PHF contains a higher fraction of α-helix than soluble tau and that the fractions of soluble tau and PHF-tau present are strongly dependent on the properties of the buffer system used. In light of these results, it is quite possible that in 20 mM phosphate there is a higher fraction of filamentous tau present, resulting in an estimated helical fraction greater than those observed for PHF in TBS. It is also interesting that both PHF in TBS and in 20 mM phosphate undergo a cooperative thermal transition within 5 °C of one another and that both are consistent with an unraveling of the PHF helical structure.

Finally, it is somewhat puzzling as to why the CD spectra of soluble or filamentous tau isolated from human PHF does not resemble spectra previously reported for cloned tau (*33*, *34*) or those reported for tau peptides and cloned FTDP-17 tau mutant protein in helical filaments (*27*, *28*, *36*). Previous CD studies have shown that phosphorylation of cloned tau (*53*), tau peptides (*21*), and the C-terminal domain of the largest subunit of RNA polymerase II, a domain similar to tau in having a high frequency of S(T)PXX and PXXP motifs (*57*), has only a minor effect on protein conformation. We have previously reported the presence of a unique PHF-glycolipid strongly associated with PHF isolated from brain (*12*−*14*) and others have documented how lipids or phospholipids alter tau's conformation or induce filament formation (*25*, *65*). It is possible that the combined effect of phosphorylation and other nonproteinaceous components stabilize a unique conformation of tau in solution characteristic of AD pathology.

ACKNOWLEDGMENT

I would like to thank Dr. Peter Davies for his gift of immunoaffinity-purified PHF.

REFERENCES

1. Spillantini, M. G., and Goedert, M. (1998) *Trends Neurosci. 21*, 428−433.
2. Wilhelmsen, K. C. (1999) *Proc. Natl. Acad. Sci. U.S.A. 96*, 7120−7121.
3. Wischik, C. M., Crowther, R. A., Stewart, M., and Roth, M. (1985) *J. Cell Biol. 100*, 1905−1912.
4. Kidd, M. (1963) *Nature 197*, 192−193.
5. Crowther, R. A. (1991) *Proc. Natl. Acad. Sci. U.S.A. 88*, 2288−2292.
6. Crowther, R. A., and Wischik, C. M. (1985) *EMBO J. 4*, 3661−3665.
7. Brion, J. P., Passareiro, H., Nunez, J., and Flament-Durand, J. (1985) *J. Arch. Biol. 95*, 229−235.
8. Wood, J. G., Mirra, S. S., Pollock, N. J., and Binder, L. I. (1986) *Proc. Natl. Acad. Sci. U.S.A. 83*, 4040−4043.
9. Kosik, K. S., Joachim, C. L., and Selkoe, D. J. (1986) *Proc. Natl. Acad. Sci. U.S.A. 83*, 4044−4048.
10. Iqbal, K., Grundke-Iqbal, I., Smith, A. J., George, L., Tung, Y. C., and Zaidi, T. (1989) *Proc. Natl. Acad. Sci. U.S.A. 86*, 5646−5650.
11. Lee, V. M. Y., Balin, B. J., Otvos, L., Jr., and Trojanowski, J. Q. (1991) *Science 251*, 675−678.
12. Goux, W. J., Liu, B., Shumburo, A. M., Parikh, S., and Sparkman, D. R. (2001) *J. Alz. Dis. 3*, 455−466.
13. Goux, W. J., Rodriguez, S., and Sparkman,D. R. (1996) *J. Neurochem. 67*, 723−733.
14. Goux, W. J., Rodriguez, S., and Sparkman, D. R. (1995) *FEBS Lett. 366*, 81−85.
15. Biernat, J., Gustke, N., Drewes, G., Mandelkow, E. M., and Mandelkow, E. (1993) *Neuron 11*, 153−163.
16. Trinczek, B., Biernat, J., Baumann, K., Mandelkow, E. M., and Mandelkow, E. (1995) *Mol. Biol. Cell 6*, 1887−1902.
17. Wang, J. Z., Gong, C. X., Zaidi, T., Grundke-Iqbal, I., and Iqbal, K. (1995) *J. Biol. Chem. 270*, 4854−4860.
18. Mandelkow, E. M., Biernat, J., Drewes, G., Gustke, N., Trinczek, B., and Mandelkow, E. (1995) *Neurobiol. Aging 16*, 355−362.
19. Khatoon, S., Grundke-Iqbal, I., and Iqbal, K. (1992) *J. Neurochem. 59*, 750−753.
20. Hagestedt, T., Lichtenberg, B., Wille, H., Mandelkow, E. M., and Mandelkow, E. (1989) *J. Cell Biol. 109*, 1643−1651.
21. Daly, N. L., Hoffmann, R., Otvos, L., Jr., and Craik, D. J. (2000) *Biochemistry 39*, 9039−9046.
22. Wille, H., Drewes, G., Biernat, J., Mandelkow, E. M., and Mandelkow, E. (1992) *J. Cell Biol. 118*, 573−584.
23. Crowther, R. A., Olesen, O. F., Jakes, R., and Goedert, M. (1992) *FEBS Lett. 309*, 199−202.
24. Wilson, D. M., and Binder, L. I. (1995) *J. Biol. Chem. 270*, 24306−24314.
25. Wilson, D. M., and Binder, L. I. (1997) *Am. J. Pathol. 150*, 2181−2195.
26. Goedert, M., Jakes, R., Spillantini, M. G., Hasegawa, M., Smith, M. J., and Crowther, R. A. (1996) *Nature 383*, 550−553.
27. Barghorn, S., Zheng-Fischhofer, Q., Ackmann, M., Biernat, J., von Bergen, M., Mandelkow, E. M., and Mandelkow, E. (2000) *Biochemistry 39*, 11714−11721.
28. von Bergen, M., Barghorn, S., Li, L., Marx, A., Biernat, J., Mandelkow, E. M., and Mandelkow, E. (2001) *J. Biol. Chem.* 48165−48174.
29. Carmel, G., Mager, E. M., Binder, L. I., and Kuret, J. (1996) *J. Biol. Chem. 271*, 32789−32795.
30. Weaver, C. L., Espinoza, M., Kress, Y., and Davies, P. (2000) *Neurobiol. Aging 21*, 719−727.
31. Jicha, G. A., Bowser, R., Kazam, I. G., and Davies, P. (1997) *J. Neurosci. Res. 48*, 128−132.
32. Jicha, G. A., Lane, E., Vincent, I., Otvos, L., Jr., Hoffmann, R., and Davies, P. (1997) *J. Neurochem. 69*, 2087−2095.
33. Cleveland, D. W., Hwo, Y., and Kirschner, M. W. (1977) *J. Mol. Biol. 116*, 227−247.
34. Schweer, O., Schonbrunn-Hanebeck, E., Marx, A., and Mandelkow, E. (1994) *J. Biol. Chem. 269*, 24290−24297.
35. Jicha, G. A., Rockwood, J. M., Berenfeld, B., Hutton, M., and Davies, P. (1999) *Neurosci. Lett. 260*, 153−156.
36. von Bergen, M., Friedhoff, P., Biernat, J., Heberle, J., Mandelkow, E. M., and Mandelkow, E. (2000) *Proc. Natl. Acad. Sci. U.S.A. 97*, 5129−5134.
37. Sadqi, M., Hernandez, F., Pan, U., Perez, M., Schaeberle, M. D., Avila, J., and Munoz, V. (2002) *Biochemistry 41*, 7150−7155.
38. Vincent, I. J., and Davies, P. (1992) *Proc. Natl. Acad. Sci. U.S.A. 89*, 2878−2882.
39. Jicha, G. A., O'Donnell, A., Weaver, C., Angeletti, R., and Davies, P. (1999) J. *Neurochem. 72*, 214−224.
40. Laemmli, U. K. (1970) *Nature 227*, 680−685.
41. Sreerama, N., and Woody, R. W. (2000) *Anal. Biochem. 287*, 252−260.
42. Sreerama, N., Venyaminov, S. Y., and Woody, R. W. (2001) *Anal. Biochem. 299*, 271−274.
43. Ksiezak-Reding, H., Liu, W. K., and Yen, S. H. (1992) *Brain Res. 597*, 209−219.
44. Ruben, G. C., Iqbal, K., Grundke-Iqbal, I., Wisniewski, H. M., Ciardelli, T. L., and Johnson, J. E., Jr. (1991) *J. Biol. Chem. 266*, 22019−22027.
45. Hoffman, R., Lee, V. M. Y., Leight, S., Varga, I., and Otvos, L., Jr. (1997) *Biochemistry 36*, 8114−8124.
46. Daly, N. L., Hoffmann, R., Otvos, L., Jr., and Craik, D. J. (2000) *Biochemistry 39*, 9039−9046.
47. Woody, R. W. (1996) in *Circular Dichroism and the Conformational Analysis of Biomolecules* (Fasman, G. D., Ed.), pp 25−67, Plenum Press, New York.
48. Woody, R. W. (1985) in *The Peptides*, v.7 (Hruby, V. J., Ed.) pp 14−114, Academic Press, Orlando, FL.
49. Park, S. H., Shalongo, W., and Stellwagen, E. (1997) *Protein Sci. 6*, 1694−1700.
50. Woody, R. W. (1974) in *Peptides, Polypeptides and Proteins; Proceedings of the 2nd Rehovot Symposium* (Blout, E. R., Bovey, F. A., Lofan, N., and Goodman, M., Eds.) pp 338−350, Wiley Press, New York.
51. Drake, A. F., Siligardi, G., and Gibbons, W. A. (1988) *Biophys. Chem. 31*, 143−146.
52. Schweers, O., Mandelkow, E. M., Biernat, J., and Mandelkow, E. (1995) *Proc. Natl. Acad. Sci. U.S.A. 92*, 8463−8467.

53. Schneider, A., Biernat, J., von Bergen, M., Mandelkow, E., and Mandelkow, E. M. (1999) *Biochemistry 38*, 3549−3558.
54. Ghoshal, N., Garcia-Sierra, F., Fu, Y., Beckett, L. A., Mufson, E. J., Kuret, J., Berry, R. W., and Binder, L. I. (2001) *J. Neurochem. 77*, 1372−1385.
55. Booth, D. R., Sunde, M., Bellotti, V., Robinson, C. V., Hutchinson, W. L., Fraser, P. E., Hawkins, P. N., Dobson, C. M., Radford, S. E., Blake, C. C. R., and Pepys, M. B. (1997) *Nature 385*, 787−793.
56. Urry, D. W., Long, M. M., Ohnishi, T., and Jacobs, M. (1974) *Biochem. Biophys. Res. Commun. 61*, 1427−1433.
57. Bienkiewicz, E. A., Woody, A. Y. M., and Woody, R. W. (2000) *J. Mol. Biol. 297*, 119−133.
58. Liu, W. K., Ksiezak-Reding, H., and Yen, S. H. (1991) *J. Biol. Chem. 266*, 21723−21727.
59. Suzuki, M. (1989) *J. Mol. Biol. 207*, 61−84.
60. Chou, P. Y., and Fasman, G. D. (1978) *Adv. Enzymol. Relat. Areas Mol. Biol. 47*, 45−148.
61. Gierasch, L. M., Deber, C. M., Madison, V., Niu, C. H., and Blout, E. R. (1981) *Biochemistry 20*, 4730−4738.
62. Bandekar, J., Evans, D. J., Krimm, S., Leach, S. J., Lee, S., McQuie, J. R., Minasian, E., Nemethy, G., Pottle, M. S., Scheraga, H. A., Stimson E. R., and Woody, R. W. (1982) *Int. J. Peptide Protein Res. 19*, 187−205.
63. Bush, C. A., Sarkar, S. K., and Kopple, K. D. (1978) *Biochemistry 17*, 4951−4954.
64. Lu, P. J., Wulf, G., Zhou, X. Z., Davies, P., and Lu, K. P. (1999) *Nature 399*, 784−788.
65. Shea, T. B. (1997) *J. Neurosci. Res. 50*, 114−122.

BI016079H